Phys Chem Minerals (2002) 29: 663–667
DOI 10.1007/s00269-002-0280-4

ORIGINAL PAPER

S. Klemme · J. C. van Miltenburg

Thermodynamic properties of nickel chromite ($NiCr_2O_4$) based on adiabatic calorimetry at low temperatures

Received: 13 August 2002 / Accepted: 6 October 2002

Abstract The hitherto unknown low-temperature heat capacity of nickel chromite ($NiCr_2O_4$) was measured between 8 and 381 K using adiabatic calorimetry, and some thermochemical functions [$C_P(T)$, $S(T)$, $S°_{298}$, $H_{(T)}-H_{(0)}$] were derived from the results. The standard entropy ($S°_{298} = 140.0 \pm 0.3$ J mol^{-1} K^{-1}) for nickel chromite was calculated from the results. Our calorimetric measurements indicate three major anomalies in the heat-capacity curve at temperatures between 8 and 381 K. A short literature review indicates that two of these anomalies can be accounted for, whereas an anomaly peaking at 29 K has not been reported previously.

Keywords Nickel chromite · $NiCr_2O_4$ · Heat capacity · Low-temperature calorimetry

Introduction

Chromium spinels are common mineral phases in the Earth's mantle and crust (e.g. Ringwood 1975). Furthermore, chromium spinels have also found frequent application in materials science. For example, nickel chromite ($NiCr_2O_4$) spinels are commonly used as catalytic materials (e.g. Jebarathinam et al. 1994; Vivekanandan G. and Krishnasamy 1995; Sloczynski et al. 1999; Dubey et al. 2001), gas sensors (Honeybourne and Rasheed 1996) and occur as high-temperature oxidation products of Ni-containing alloys (e.g. Strawbridge 1993). Thermodynamic properties of chromium spinels have therefore been investigated by numerous studies in both Earth sciences (e.g. Irving 1965, 1967; Sack and Ghiorso 1991) and in materials science (e.g. Mülller and Kleppa 1973; Park and Kim 1999). Although some progress has been made to understand complex chromian spinel solid solutions (e.g. Oka et al. 1984; Sack and Ghiorso 1991; Park and Kim 1999; Klemme and O'Neill 1997), there is still a lack of fundamental thermodynamic data for many spinels of end-member composition (cf. Klemme et al. 2000; Klemme and van Miltenburg 2003; Ehrenberg et al. 2002), which should be well known before attempting to understand complex solid solutions.

This is the case for $NiCr_2O_4$. Nickel chromite ($NiCr_2O_4$) is a normal spinel with Ni^{2+} occupying the slightly distorted A sites and Cr^{3+} solely occuping the B sites (Romeijn 1953). Two magnetic and structural transitions in $NiCr_2O_4$ were reported from the literature. The cubic-tetragonal phase transition at around 300 K has been well studied and is commonly interpreted as caused by a Jahn-Teller distortion of magnetic ions (Lotgering 1956; Kino et al. 1972; Armbruster et al. 1983; Crottaz et al. 1997; Ueno et al. 1999). A further magnetic transition has been observed at somewhat lower temperatures between 60 and 80 K (McGuire et al. 1952; Lotgering 1956; Prince 1961; Tsushima 1962; Göring et al. 1978; Armbruster et al. 1983). There is only little known about the structure of $NiCr_2O_4$ at even lower temperatures (Prince 1961). Moreover, there are no previous low-temperature heat capacity measurements for $NiCr_2O_4$ available in the literature. Existing values for the standard entropy of $NiCr_2O_4$ at 298.15 K were only estimated (e.g. Kubaschewski et al. (1993) [$S°_{298.15} = 124.3 \pm 8.4$ J mol^{-1} K^{-1}] and are probably too low.

To further address the afore-mentioned matters, we performed low-temperature calorimetric measurements to investigate the heat capacity of $NiCr_2O_4$ between 8 and 381 K.

S. Klemme (✉)
Mineralogisches Institut, Universität Heidelberg,
Im Neuenheimer Feld 236, 69120 Heidelberg, Germany
email: sklemme@min.uni-heidelberg.de

J.C. van Miltenburg
Thermodynamic Centre, Utrecht University,
Padualaan 8, 3584 CH, Utrecht, The Netherlands

Experimental

Sample preparation and characterization

Heat-capacity measurements were performed on synthetic polycrystalline nickel chromite samples. Ni (purity 99.99%) and Cr_2O_3

(purity 99.99%) were mixed in appropriate proportions in an agate mortar under acetone. The mixture was then pressed into pellets (1 cm diameter) and sintered in a conventional vertical furnace at atmospheric pressure and 1200 °C for 24 h in air. The pellets were subsequently quenched in air. The samples were then reground, repressed and reannealed under identical conditions. X-ray diffraction indicated $NiCr_2O_4$ only; no impurities or unreacted oxides were detected. Lattice parameters of our synthetic nickel chromite were found to be $a = 5.8340(11)$ Å, $c = 8.4232(9)$ Å, which compares reasonably well with previous results (Armbruster et al. 1983; Crottaz et al. 1997; Ueno et al. 1999). The pellets weighed 8.35 g.

Low-temperature calorimetry

The calorimeter used, laboratory designation CAL V, has been described before (van Miltenburg et al. 1987). More recent improvements in design and data handling were described recently (van Miltenburg et al. 1998). Temperature was measured with a calibrated 27 ohm Rh/Fe thermometer (calibration by Oxford Instruments with an accuracy of about 0.001 K), using an automated AC bridge (Tinsley). The thermometer scale applied was the ITS-90 scale (Preston-Thomas 1990). The sample was broken into several grains of about 2 mm. A helium pressure of 1000 Pa was established to the sample chamber to promote heat exchange. Measurements were made in the intermittent mode. Several measurements were made, starting with a series from 296 to 381 K. As no influence of the thermal history on the data could be detected, all series were combined in one file, except one which was made with temperature increments of about 0.7 K to investigate the fine structure around 310 K. Stabilization periods of about 500 s were used in between the heating periods. Below 30 K, the periods were in the order of 150 s. Below 30 K, the reproducibility of the calorimeter is about

Table 1 Experimental molar heat capacities for $NiCr_2O_4$

Temperature (K)	C_P (J mol^{-1} K^{-1})	Temperature (K)	C_P (J mol^{-1} K^{-1})	Temperature (K)	C_P (J mol^{-1} K^{-1})	Temperature (K)	C_P (J mol^{-1} K^{-1})
8.04	0.48	53.50	23.59	170.55	89.55	287.15	137.07
8.50	0.54	56.04	25.34	173.26	90.91	289.32	137.94
9.64	0.86	58.62	27.13	175.94	92.28	296.74	141.35
9.91	0.86	61.22	29.11	178.60	93.60	297.80	141.45
10.53	1.07	63.84	31.19	181.24	94.93	299.33	142.26
11.06	1.24	66.48	33.30	183.86	96.15	301.32	143.46
11.86	1.41	69.17	33.43	186.46	97.45	303.31	145.45
12.19	1.62	71.92	33.68	189.04	98.68	305.28	147.77
12.74	1.77	74.69	34.82	191.61	99.89	307.26	149.32
13.48	2.03	77.45	36.24	194.16	101.09	309.24	149.29
13.95	2.26	80.22	37.79	196.69	102.24	311.23	150.05
14.56	2.54	83.00	39.38	199.21	103.40	313.22	147.42
15.27	3.08	83.91	39.91	201.72	104.51	315.23	144.81
15.97	3.27	85.43	40.80	204.21	105.65	317.25	141.10
16.46	3.78	85.79	40.98	206.68	106.72	319.27	138.18
17.18	4.11	87.61	42.09	209.15	107.79	321.29	137.92
18.00	4.80	88.54	42.58	211.60	108.85	323.28	138.22
18.41	5.12	90.45	43.76	214.03	109.86	325.27	138.68
19.14	5.78	91.22	44.16	216.46	110.92	327.26	139.01
20.04	6.78	93.27	45.39	218.88	111.90	329.24	139.44
20.43	7.16	93.81	45.68	221.28	112.91	331.23	139.83
21.16	7.97	96.09	47.04	223.67	113.86	333.22	140.22
22.17	9.34	96.34	47.17	226.05	114.85	335.20	140.58
22.53	9.73	98.81	48.64	228.42	115.76	337.19	140.96
23.27	10.72	98.92	48.71	230.78	116.68	339.18	141.33
24.37	12.47	101.77	50.69	233.13	117.60	341.17	141.73
24.70	12.82	104.61	52.15	235.47	118.48	343.15	142.02
25.46	14.03	107.47	54.05	237.80	119.40	345.14	142.45
26.69	15.92	110.33	55.72	240.13	120.32	347.13	142.82
26.99	15.94	113.20	57.33	242.44	121.14	349.12	143.14
27.80	16.49	116.08	58.95	244.75	122.00	351.11	143.46
29.23	16.98	118.96	60.61	247.04	122.80	353.11	143.80
29.52	16.50	121.84	62.09	249.33	123.66	355.10	144.17
30.14	15.89	124.73	64.07	251.61	124.58	357.09	144.57
32.19	14.57	127.62	65.78	253.88	125.08	359.08	144.94
32.29	14.34	130.52	67.47	256.15	125.77	361.08	145.17
32.32	14.22	133.43	69.17	258.41	126.66	363.07	145.44
34.32	14.32	136.34	70.82	260.66	127.48	365.06	145.84
34.95	14.49	139.25	72.50	262.91	128.29	367.06	146.20
35.28	14.81	142.17	74.16	265.15	129.14	369.05	146.55
36.12	14.80	145.09	75.81	267.38	129.94	371.05	146.81
37.77	15.02	148.01	77.47	269.60	130.70	373.04	147.14
38.06	15.37	150.93	79.07	271.82	131.48	375.04	147.45
39.30	15.62	153.82	80.65	274.03	132.25	377.03	147.68
40.51	16.32	156.68	82.23	276.23	133.05	379.03	148.07
43.17	17.81	159.51	83.74	278.43	133.86	381.03	148.33
45.98	19.06	162.31	85.23	280.62	134.53		
48.52	20.54	165.08	86.68	282.80	135.35		
50.98	21.99	167.83	88.14	284.98	136.23		

Table 2 Experimental molar heat capacities for $NiCr_2O_4$ around the cubic-tetragonal transition

Temperature (K)	C_P ($J\ mol^{-1}K^{-1}$)	Temperature (K)	C_P ($J\ mol^{-1}K^{-1}$)
290.81	137.94	311.42	149.79
291.50	138.30	312.09	149.18
292.20	138.46	312.77	147.78
292.89	138.77	313.45	146.48
293.59	139.18	314.13	145.62
294.28	139.41	314.82	144.97
294.98	139.79	315.50	144.04
295.67	140.11	316.19	142.28
296.36	140.57	316.87	141.02
297.06	140.95	317.57	140.02
297.75	141.10	318.26	138.80
298.44	141.47	318.95	137.74
299.13	141.81	319.65	137.21
299.82	142.23	320.35	137.38
300.51	142.47	321.04	137.62
301.20	142.91	321.74	137.54
301.89	143.41	322.44	137.66
302.58	143.98	323.13	137.93
303.27	144.41	323.83	137.95
303.95	145.04	324.53	138.17
304.64	146.32	325.22	138.33
305.32	147.31	325.92	138.52
306.00	148.28	326.61	138.68
306.68	148.60	327.30	138.62
307.36	148.85	328.00	138.91
308.03	148.69	328.69	138.94
308.71	148.44	329.39	139.33
309.39	148.74	330.08	139.09
310.07	148.77	330.77	139.35
310.74	149.37	331.47	139.58

1%, between 30 and 100 K 0.05–0.1% and above 100 K 0.03%. Checking the calorimeter with standard materials (*n*-heptane and synthetic sapphire) showed no deviations larger than 0.2% from the recommended values.

Results and discussion

The experimental values for the low-temperature heat capacity of nickel chromite are compiled in Tables 1 and 2. The values have been corrected for the contribution of the empty calorimeter. The experimental data were interpolated at every degree to calculate S_{abs} and $H_{(T)}-H_{(0)}$ by numerical integration, and are given in Table 3. The starting values for the entropy and the enthalpy were calculated assuming that below 10 K the Debye law ($C_P = \alpha T^3$) is followed. From our data we suggest a value for $\alpha = 8.807 \times 10^{-4}$ J K^{-4} mol^{-1}.

Figure 1 depicts the heat capacity of $NiCr_2O_4$ as a function of temperature. A large anomaly in the heat-capacity curve is observed at around 310 K. This is interpreted to be the cubic-tetragonal phase transition which has been investigated previously by a number of studies (Prince 1961; Kino et al. 1972; Armbruster et al. 1983; Inaba et al. 1986; Crottaz et al. 1997; Ueno et al. 1999). It seems to be generally accepted that this transition is caused by a cooperative Jahn–Teller effect. Our transition temperature lies well within the range of those reported by these studies. Detailed studies of the transition (three heat-capacity scans altogether) confirm two discrete peaks, as expected for a first-order transition (Fig. 2). At lower temperatures we find another heat-capacity anomaly peaking at about 70 K (Fig. 3). We interpret this anomaly to be related to the ferrimagnetic–ferromagnetic transition which has been reported previously by a number of authors. For example, Lotgering (1956) reports this transition at around 80 K, whereas results by Prince (1961), Tsushima (1962) and Armbruster et al. (1983) indicate that the transition occurs at

Table 3 Thermodynamic properties at selected temperatures for $NiCr_2O_4$. Molar mass = 226.683 g mol^{-1}

Temperature (K)	C_P ($JK^{-1}\ mol^{-1}$)	S ($JK^{-1}\ mol^{-1}$)	$H_{(T)}-H_{(0)}$ ($J\ mol^{-1}$)
10	0.8897	0.2960	2.220
15	2.871	0.9613	10.73
20	6.742	2.259	33.73
25	13.29	4.418	82.70
30	16.01	7.253	160.51
35	14.52	9.555	235.08
40	16.03	11.60	312.04
45	18.59	13.69	400.48
50	21.41	15.77	499.47
55	24.62	17.96	614.47
60	28.16	20.25	746.36
65	32.12	22.66	897.17
70	33.49	25.12	1063
75	34.98	27.47	1233
80	37.67	29.81	1415
85	40.55	32.18	1610
90	43.49	34.60	1822
95	46.39	37.02	2046
100	49.45	39.49	2287
105	52.40	41.97	2541
110	55.53	44.48	2811
120	61.15	49.55	3394
130	67.17	54.69	4036
140	72.93	59.88	4737
150	78.57	65.10	5494
160	84.00	70.34	6307
170	89.27	75.59	7173
180	94.31	80.84	8091
190	99.13	86.07	9058
200	103.75	91.27	10073
210	108.16	96.44	11133
220	112.37	101.57	12235
230	116.37	106.65	13379
240	120.27	111.69	14562
250	123.93	116.67	15783
260	127.24	121.59	17038
270	130.84	126.46	18329
280	134.33	131.29	19655
290	138.22	136.07	21017
298.15	141.62	139.95	22159
300	142.63	140.83	22422
310	149.79	145.64	23891
320	137.88	150.23	25336
330	139.59	154.50	26722
340	141.49	158.70	28128
350	143.28	162.82	29552
360	145.06	166.88	30994
370	146.68	170.88	32452

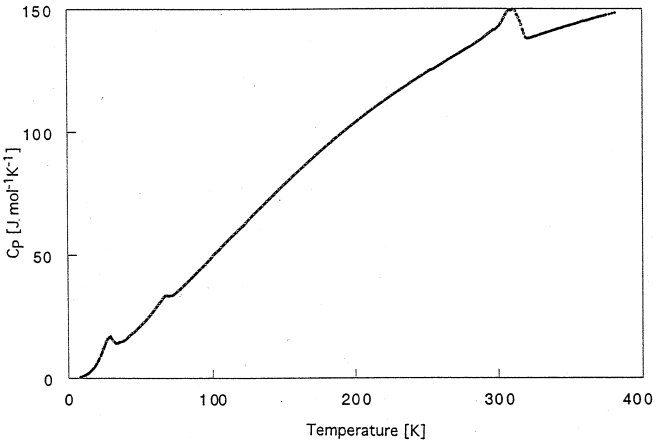

Fig. 1 The heat capacity of polycristalline $NiCr_2O_4$ (nickel chromite) measured between 8 and 380 K. Three heat-capacity anomalies are observed at around 310 and 75 and at 29 K, respectively. The broad anomaly around 310 K coincides with the cubic-tetragonal phase transition of $NiCr_2O_4$ reported previously. See text for details and discussion

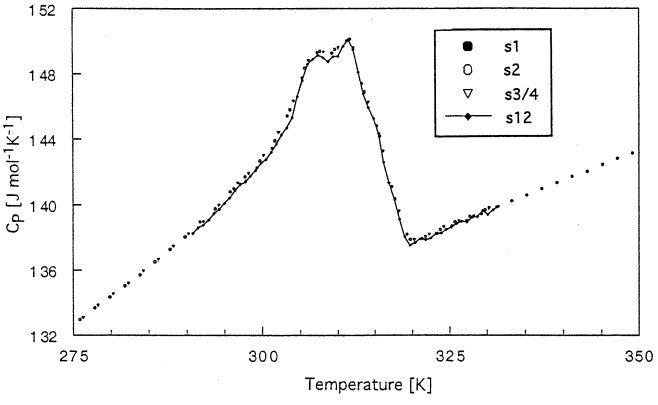

Fig. 2 An enlarged view of the high-temperature part of the experimental data. Depicted are results of four scans over the transition around 310 K. *Series S 12* was made in steps of 0.7 K

around 65 K. Furthermore, Armbruster et al. (1983) report an orthorhombic structure of $NiCr_2O_4$ at temperatures below 65 K.

At even lower temperatures, however, we observe another lambda-shaped heat-capacity anomaly peaking at 29 K (Fig. 3). This anomaly has not been reported previously. Figure 4 shows that our heat capacity data follow Debye's law from 0 K up to about 27 K, then the afore-mentioned low-temperature heat-capacity anomaly hits in. The standard entropy at 298.15 K (S°_{298}) was calculated from the C_P data (using a T^3 extrapolation to 0 K) and resulted in $S^\circ_{298} = 140.0 \pm 0.3$ J mol^{-1} K^{-1}, which is substantially higher than the estimated values of Kubaschewski et al. (1993).

Acknowledgements Many thanks to reviewers Drs. B.S. Hemingway and E.F. Westrum, who helped to improve the manuscript.

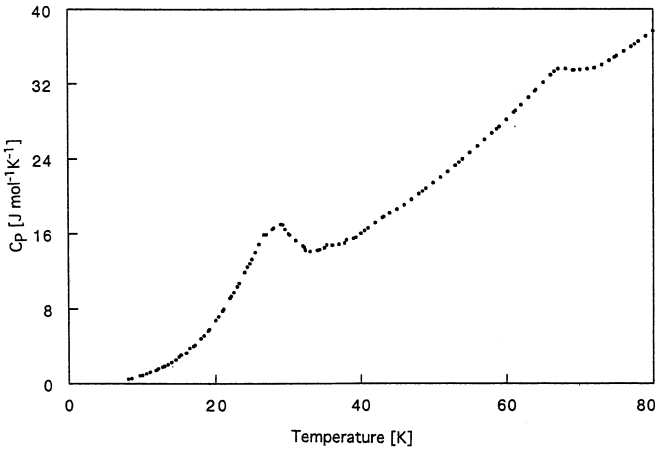

Fig. 3 An enlarged view of the low-temperature part of the experimental data. A small anomaly is observed peaking at about 75 K. This is probably due to a ferrimagnetic to ferromagnetic transition in $NiCr_2O_4$, see text for details. The data reveal another broader anomaly which peaks at 29 K indicative of further, presumably magnetic, ordering at very low temperatures. The latter anomaly has not been reported previously

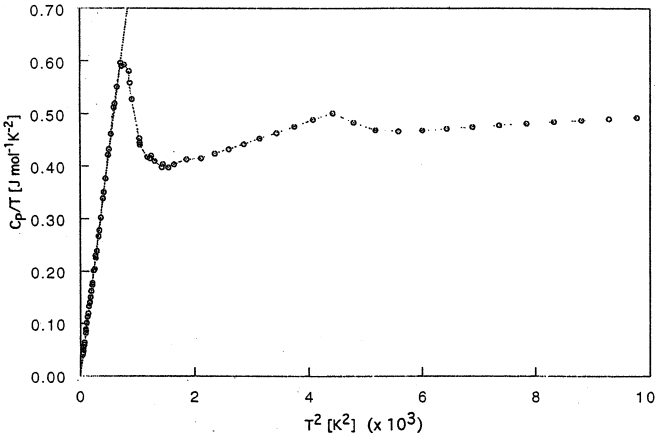

Fig. 4 A plot of C_P/T against T^2. Our results indicate that the heat capacity follows the low-temperature Debye law ($C_P = \alpha T^3$) at temperatures between 0 and 27 K, then a sudden change takes place and the effects of a low-temperature heat-capacity anomaly are observed

References

Armbruster T, Lager GA, Ihringer J, Rotella FJ, Jorgensen JD (1983) Neutron and X-ray-powder study of phase transitions in the spinel $NiCr_2O_4$. Z Kristallogr 162: 8–10

Crottaz O, Kubel F, Schmid H (1997) Jumping crystals of the spinels $NiCr_2O_4$ and $CuCr_2O_4$. J Mat Chem 7: 143–146

Dubey BL, Singh NB, Srivastava JN, Ojha AK (2001) The catalytic behaviour of $NiFe_{2-x}Cr_xO_4$ ($0.0 <= x <= 2.0$) during the thermal decomposition of ammonium perchlorate, polystyrene and their composite propellants. Indian J Chem 40: 841–847

Ehrenberg H, Knapp M, Baehtz C, Klemme S (2002) Tetragonal low-temperature phase of $MgCr_2O_4$. Powder Diff 17: 230–233

Göring J, Wurtinger W, Link R (1978) ^{61}Ni Mössbauer-effect studies of the hyperfine interaction in the magnetic spinel $NiCr_2O_4$. J Appl Phys 49: 269–272

Honeybourne CL, Rasheed RK (1996) Nitrogen dioxide and volatile sulfide sensing properties of copper, zinc and nickel chromite. J Mat Chem 6: 277–283

Inaba H, Yagi H, Naito K (1986) Heat-capacity anomalies due to the cooperative Jahn–Teller effect in $Cu_{1-x}Ni_xCr_2O_4$. J Solid State Chem 64: 67–75

Irvine TN (1965) Chromian spinel as a petrogenetic indicator I: theory. Can J Earth Sci 2: 648–672

Irvine TN (1967) Chromian spinel as a petrogenetic indicator II: petrologic applications. Can J Earth Sci 4: 71–103

Jebarathinam NJ, Eswaramoorthy M, Krishnasamy V (1994) Dehydrogenation of ethylbenzene over spinel oxides. Bull Chem Soc Japan 67: 3334–3338

Kino Y, Lüthi B, Mullen ME (1972) Cooperative Jahn–Teller phase transition in the nickel-zinc-chromite system. J Phys Soc Japan 33: 687–697

Klemme S, O'Neill HStC (1997) The reaction $MgCr_2O_4 + SiO_2 = Cr_2O_3 + MgSiO_3$ and the free energy of formation of magnesiochromite ($MgCr_2O_4$). Contrib Mineral Petrol 130: 59–65

Klemme S, van Miltenburg JC (2003) Thermodynamic properties of hercynite ($FeAl_2O_4$) based on adiabatic calorimetry at low temperatures. Am Mineral (in press)

Klemme S, O'Neill HStC, Schnelle W, Gmelin E (2000) The heat capacity of $MgCr_2O_4$, $FeCr_2O_4$ and Cr_2O_3 at low temperatures and derived thermodynamic properties. Am Mineral 85: 1686–1693

Kubaschewski O, Alcock CB, Spencer PJ (1993) Materials thermochemistry. Pergamon Press, Oxford

Lotgering FK (1956) On the ferromagnetism of some spinels sulphides and oxides. II. Oxygen and sulphur spinels containing chromium (MCr_2O_4 and MCr_2S_4). Philips Res Rept 11: 218–249

McGuire TR, Howard LN, Smart JS (1952) Magnetic properties of the chromites. Ceramic Age 60: 22–24

Müller F, Kleppa OJ (1973) Thermodynamics of formation of chromite spinels. J Inorg Nucl Chem 35: 2673–2678

Oka Y, Steinke P, Chatterjee ND (1984) Thermodynamic mixing properties of $Mg(Al,Cr)_2O_4$ spinel crystalline solutions at high pressures and temperatures. Contrib Mineral Petrol 87: 196–204

Park B-H, Kim D-S (1999) Thermodynamic properties of Ni-Cr_2O_4–$NiFe_2O_4$ spinel solid solution. Bull Korean Chem Soc 20: 939–942

Preston–Thomas H (1990) The international temperature scale of 1990 (ITS-90). Metrologia 27: 3–10

Prince E (1961) Structure of nickel chromite. J Appl Phys 32 (Supplement): 68–69

Ringwood AE (1975) Composition and petrology of the Earth's mantle. McGraw-Hill, New York

Romeijn FC (1953) Physical and crystallographical properties of some spinels. Philips Res Rep 8: 304–320

Sack RO, Ghiorso MS (1991) Chromian spinels as petrogenetic indicators: Thermodynamics and petrological applications. Am Mineral 76: 827–847

Sloczynski J, Ziolkowski J, Grzybowska B, Grabowski R, Jachewicz D, Wcislo K, Gengembre L (1999) Oxidative dehydrogenation of propane on $Ni_xMg_{1-x}Al_2O_4$ and $NiCr_2O_4$ spinels. Journal of Catalysis 187: 410–418

Strawbridge A, Stott FH, Wood GC (1993) The formation and incorporation into the scale of internal oxides developed during the high-temperature oxidation of dilute nickel-base alloys. Corrosion Science 35: 852–855

Tsushima T (1962) Magnetic properties and crystal chemistry of nickel chromite single crystals. J Phys Soc Japan 17: 189

Ueno G, Sato S, Kino Y (1999) The low-temperature tetragonal phase of $NiCr_2O_4$. Acta Cryst (C) 55: 1963–1966

van Miltenburg JC, van den Berg GJK, van Bommel MJ (1987) Construction of an adiabatic calorimeter. Measurements of the molar heat capacity of synthetic sapphire and of *n*-heptane. J Chem Thermodyn 19: 1129–1137

van Miltenburg JC, van Genderen ACG, van den Berg GJK (1998) Design improvements in adiabatic calorimetry. The heat capacity of cholesterol between 10 and 425 K. Thermochim Acta 319: 151–162

Vivekanandan G, Krishnasamy V (1995) Catalytic transformations of phenethyl alcohols in the vapor phase. Hung J Ind Chem 23: 21–26